RSC Advances

ROYAL SOCIETY OF CHEMISTRY

www.rsc.org/advances

Journal Name

RSCPublishing

ARTICLE

Exploring the potential of exfoliated ternary ultrathin Ti_4AlN_3 nanosheets for fabricating hybrid patterned polymer brushes

Cite this: DOI: 10.1039/xoxxoooooox

Received ooth January 2012,
Accepted ooth January 2012

DOI: 10.1039/xoxxoooooox

www.rsc.org/

Qun Ye,[#a] Peng Xiao,[#a] Wulong Liu,[a] Ke Chen,[a] Tao Chen,[*a] Jianming Xue,[b] Shiyu Du[a] and Qing Huang[*a]

Since the discovery of graphene, two-dimensional (2D) materials have been receiving increased attention. The quest for new 2D materials with unique structure and special properties becomes urgent. Herein we report on the preparation of a new kind of ternary 2D material, Ti_4AlN_3 nanosheets by liquid exfoliating of the corresponding laminated MAX phase. The obtained Ti_4AlN_3 nanosheets, bearing abundant surface groups, can be further used to fabricate micro-patterns via micro-contact printing (μCP) and subsequently functionalized through self-initiated photografting and photopolymerization (SIPGP) to achieve MAX-based hybrid patterned polymer brushes. Our work opens a door to explore the synthesis of 2D hybrid materials for functional applications basing on the traditional MAX phases.

Introduction

Two-dimensional (2D) materials have garnered tremendous interest recently. They offer high specific surface area, diverse electronic structure and properties compared with their bulk counterparts. Among typical 2D materials, graphene is arguably the most studied due to its unique mechanical, thermal, electronic, and optical properties.[1] Other 2D materials containing two elements, such as hexagonal boron nitride (*h*-BN),[2, 3] transition metal dichalcogenides,[4] and metal oxides,[5] have also been receiving increased attention. Recently, a new family of binary 2D materials, named as MXenes, was reported.[6] They were produced by etching of A elements from MAX, or $M_{n+1}AX_n$ phases (M is an early transition metal, A is mainly an A-group element, X is carbon and/or nitrogen, and n = 1, 2, or 3)[7-9] by F-contained etchants (HF, NH_4HF_2,[10] or the mixture[11] of fluoride salts and hydrochloric acid), leaving $M_{n+1}X_n$ layers. By far the MXene family includes Ti_3C_2, Ti_2C, $(Ti_{0.5}, Nb_{0.5})_2C$, $(V_{0.5}, Cr_{0.5})_3C_2$, Ti_3CN, Ta_4C_3, Nb_2C, V_2C, and Nb_4C_3.[12-15] These MXenes have greatly enlarged the number of binary 2D materials, and showed promising performance as electrode materials in both lithium ion batteries (LIBs) and supercapacitors,[14, 16, 17] catalyst supports in the chemical industry,[18, 19] and adsorbents for heavy metal ions.[20]

These unexpected 2D materials, MXenes derived from MAX phases intrigue the exploration of multi-element graphene-like materials. In fact, in the $Ti_3Si_{0.75}Al_{0.25}C_2$ (TSAC) case, the partial solid solution of Al in Si site weakened the bond strength of A layers, and favored the formation of TSAC nanosheets.[21] Compared with ones comprising of single or binary element, these multi-element 2D materials broaden the opportunity to tune their physical and chemical properties. Moreover, the above-mentioned discovery of MXene materials only takes advantage of features of their binary MX units, not of parent ternary MAX phase, whose appealing structural and functional characters, such as excellent conductivity, good oxidation resistant,[22] and radiation tolerance,[23] have been widely studied.[7] Hence, an effective strategy to exfoliate the bulk MAX phases into 2D ones with intact crystal configuration for functional applications is highly needed.

Inspired by the exfoliation behavior of carbide MAX phase to 2D MXene[6] or MAX phase nanosheets[21], herein, we report a strategy to prepare exfoliated 2D nitride MAX nanosheets (using Ti_4AlN_3 as a sample) derived from the corresponding MAX phase by etching in diluted hydrofluoric acid (HF) with a following ultrasonic treatment. Unlike TSAC sheets[21] directly exfoliated from A-layer-activated MAX phase with ultrasound more than 12 hours, the Ti_4AlN_3 powders are firstly etched in the caustic HF solution with a suitable concentration. Many defects form in the structure due to the corrosion, and the following exfoliation process of Ti_4AlN_3 powders to nanosheets becomes easier and more efficient. In order to further explore the potential of this new 2D inorganic material, micro-patterns and chemical functionality of Ti_4AlN_3 nanosheets were attempted. After etching in HF solution, the surface of materials is usually attached by hydrophilic hydroxyl and fluorine groups.[6, 14] As an active site, -OH group has been successfully utilized to fabricate micro-patterned graphite oxide (GO) films through micro-contact printing (μCP) induced supramolecular self-assembly of GO nanosheets,[24] and initiated to grow poly(2-(dimethylamino)ethyl methacrylate) (PDMAEMA) polymer brushes via self-initiated photografting and photopolymerization (SIPGP) from V_2C MXene to achieve the "smart" properties of CO_2 and temperature dual response.[25] The fabrication of hybrid polymer brushes with controllable sizes and special properties can vastly extend the applications of the corresponding organic or inorganic material. Our work thus allows us to achieve 2D hybrid patterned polymer brushes grafted from MAX nanosheets, which will endow the traditional MAX phases to have more smart functionality.

Experimental

Materials

Ti_4AlN_3 phase used in this work was synthesized from the starting raw materials of Ti, Al, and TiN powders with a non-stoichiometric molar ratio of 1: 1.2: 2.05 by a microwave sintering method at 1250 °C for 30 min in an argon atmosphere.[26] Styrene (~99% purity, Alfa Aesar China (Tianjin) Co., Ltd) was purified by neutral Al_2O_3 column chromatography and dried with a 0.4 nm molecular sieve at room temperature for 3 days. Patterned PDMS stamps were fabricated from Sylgard 184 (the ratio between component A and B was 1: 10) on a silicon master. Silicon wafers were cleaned in a mixture of H_2O_2/H_2SO_4, 1:3 (v/v, i.e. "piranha solution") at 80 °C for 2 h and washed thoroughly with Milli-Q-grade water.

Preparation of Ti_4AlN_3 Ink

Roughly 3 g Ti_4AlN_3 powders were immersed in about 50 mL of 20 wt. % diluted HF solution at room temperature for 30 h. The etched powders were collected by centrifugal treatment and then washed several times using deionized water. To obtain stable suspension, the powders were then dispersed into alcohol and ultrasonically treated for nearly 6 h. After standing still for more than 24 h, the solution was centrifuged at about 3000 rpm to remove large-size particles, leaving a stable ink.

Micro-contact Printing (μCP)

The patterned PDMS stamp was inked by exposing the stamp features to the ink of Ti_4AlN_3 sheets for 3 min and drying with nitrogen, and then brought into contact with Si substrate for 1 min with an adequate applied force of 50 g to fabricate the patterns on the substrate.

Self-initiated Photografting and Photopolymerization[27]

The patterned Si substrates surface was submerged in 2 mL of styrene monomer and irradiated with an UV fluorescent lamp with a spectral distribution between 300 and 400 nm (λ_{max} = 365 nm with a total power of ~240 mW/cm^2) for 1 h in N_2 atmosphere. After SIPGP, the functionalized substrate were rinsed with several solvents (toluene, ethyl acetate, and ethanol for styrene) to remove physisorbed polymer.

Characterization

The phase composition of samples before and after immersion was analyzed by X-ray diffraction (XRD), using a diffractometer (D8 Advance, Bruker AXS, Germany) with Cu K_α radiation. Their microstructures were characterized by a scanning electron microscope (SEM, FEI Quanta 250 FEG, Hillsboro, OR), and transmission electron microscopy (TEM, FEI Tecnai F20) at an acceleration voltage of 200 kV. Atomic force microscopy (AFM) study in this work was taken by a multimode AFM (Being Nano-Instruments, Ltd) operating in the contact and/or tapping mode using silicon cantilevers.

Results and discussion

The preparation process of the exfoliated ternary Ti_4AlN_3 nanosheets and subsequent exploration for fabricating hybrid patterned polymer brushes is outlined in **Scheme 1**. To the best of our knowledge, it is the first effort to prepare nitride MAX nanosheets and MAX-based hybrid brushes. In order to find a suitable etching condition for exfoliation, different concentration of HF solution and etching time were initially attempted. In the diluted HF solution (i.e. 10 wt. %), the powders seemed intact due to low reaction kinetics. However, in the concentrated HF solution (i.e. 40 wt. %), Ti_4AlN_3 was vigorously eroded, and impurities such as Al_2O_3 and TiN always remained in the final products (**Figure S1, and S2**). In a moderate condition such as 20 wt. % HF for 30 h, the accordion-like structure could be easily found in the final products (**Figure 1a, and S3**). These etched products were well dispersed in water or alcohol after sonication, and formed a stable suspension even after standing still for more than 24 h (**Figure S4**). For comparison, pure Ti_4AlN_3 powders without HF-etching treatment cannot form such suspension (**Figure S4**), which is the same as the result of ultrasonic-treated Ti_3SiC_2.[21]

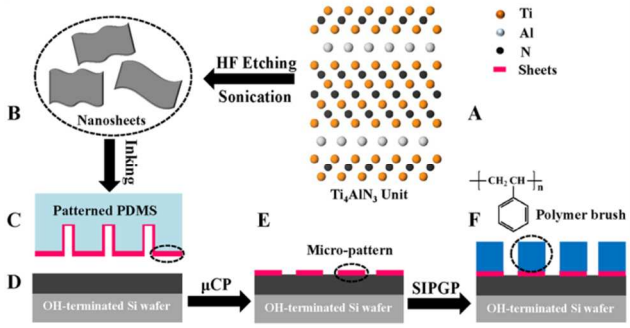

Scheme 1. Schematic procedure of preparing nitride Ti_4AlN_3 nanosheets, and subsequently fabricating hybrid patterned polymer brushes. **(A, B)** The process of etching Ti_4AlN_3 powders in the diluted hydrofluoric acid (20 wt. %) with a following ultrasonic treatment for 6 h. **(C - E)** Fabricating micro-patterns of Ti_4AlN_3 nanosheets via micro-contact printing (μCP). **(F)** Growing polymer brushes through self-initiated photografting and photopolymerization (SIPGP) on the micro-patterns.

In order to find out whether there was a successful exfoliation of Ti_4AlN_3 particles to nanosheets, scanning electronic microscopy (SEM) was employed to investigate the morphology of the products in the suspension. As shown in **Figure 1b**, sheets with a wide range of diameters from several nanometers to micrometers are obtained after sonication, which resemble the typical delaminated Ti_3C_2 MXene.[6] A transmission electron microscopy (TEM) analysis (**Figure 1c**, and **1d**) of the sheets reveals the graphene-like products are still Ti_4AlN_3 phase, which is not as-reported MXene material (i.e. Ti_4N_3 phase) as Ti_3AlC_2 phase normally does under the same etching condition. The corresponding selected area electron diffraction (SAED) pattern (**Figure 1d**) clearly reveals the hexagonal crystalline nature of the sheet, and the corresponding lattice spacing of (100), (110), and (300) planes (listed in **Figure S5a**) are all consistent with those of Ti_4AlN_3 phase. Energy dispersive spectroscopy (EDS) data (**Figure S5b**) shows the presence of Al as well as Ti and N elements, indicating the existence of Ti_4AlN_3 phase, which further corroborates the SAED result. C and Cu signals originate from the supporting foil, and vast O, F should come from the surface groups of hydroxyl and fluorine groups, which have been proved to exist in the MXene materials after HF-etching process.[6, 14] To confirm the thickness of the exfoliated sheets, tapping-mode atomic force microscopy (AFM) analysis was employed. As shows in **Figure 1e**, and **1f**, the thickness of the as-exfoliated nanosheets is only 7 - 9 nm, which is about three to four multilayers of the Ti_4AlN_3 crystal unit along c axis. The

sharp fluctuation of curves in **Figure 1f** should be due to the existence of holes or small particles on the surface of sheets.

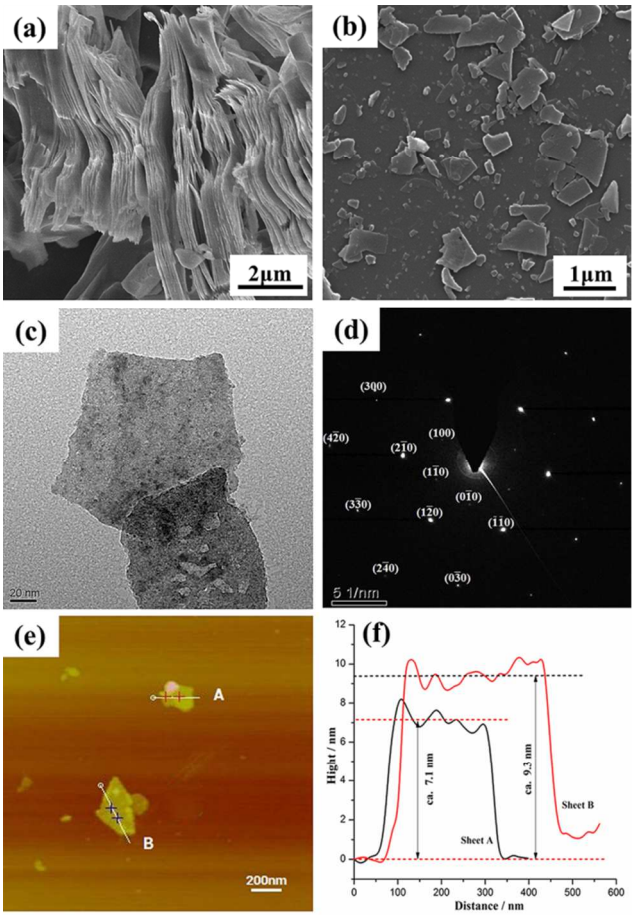

Figure 1. (a) SEM image of as-etched Ti_4AlN_3 particles in 20 wt. % HF. (b) Typical morphology of etched Ti_4AlN_3 powders after sonication for 6 h. (c) TEM image of as-obtained nanosheets, and (d) the corresponding SAED pattern. (e) AFM image of as-obtained nanosheets, and (f) the corresponding height measurement.

The formation of Ti_4AlN_3 nanosheets is further confirmed by X-ray diffraction (XRD). As **Figure 2** shows, the major phase of the exfoliated sheets (**curve C**) drying on the silicon wafer is still Ti_4AlN_3 phase (JCPDS: 65-9771), the same with the results of Ti_4AlN_3 before (**curve A**) and after (**curve B**) HF-etching treatment. However, it clearly shows that the relative intensity of peaks belonging to (00*l*) planes of Ti_4AlN_3 crystal structure increases, but the peaks assigned to (104), (105), (106) lattice planes obviously weaken. This result indicates the samples lying flat on the silicon wafer expose more basal plane (00*l*) to X-ray compared with the corresponding MAX phase powders, as SEM revealed (**Figure 1b**). Furthermore, there is still small amount of TiN phase existing in the as-prepared Ti_4AlN_3 sheets, most possibly attached on the surface of Ti_4AlN_3 nanosheets as AFM technique detected. Raman spectroscopy (**Figure S6**) also confirms the Ti_4AlN_3 phase in the products. All the characteristic Raman peaks[28] belonging to Ti_4AlN_3 phase still remained after etching and sonication. The corresponding calculated peak energies and symmetries for the assigned modes are summarized in **Table S1**.

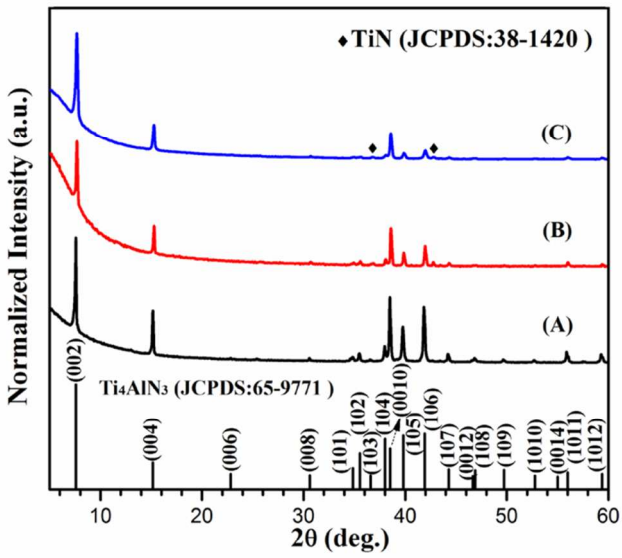

Figure 2. XRD patterns for Ti_4AlN_3 before (A) and after (B) 20 wt. % HF treatment, and for the exfoliated sheets film (C).

At present, the mechanism for the formation of ternary 2D Ti_4AlN_3 nanosheets (rather than Ti_4N_3 MXene) is not exactly known, but it could be due to the dissolution of one complete Ti_4AlN_3 unit layer (both Al and Ti_4N_3 layers) rather than single Al atom layer in HF. Since the exfoliation of MAX phases is mainly due to the active A atom (Al in all current reports on MXenes),[6, 12-15] the bond strength between A atom to M or X atom is the decisive factor to control the etching behavior in HF solution. When the X atom changes from C to N, the exfoliation behavior of MAX phase is totally different. The stronger bond[29] between Al atoms to Ti-N substructure unites the two layers, and prevents the formation of TiN_x phase in HF solution. On the contrary, Al atom is much free in the Ti_3AlC_2 phase, which well explains the formation of binary MXene materials. Furthermore, Ti_2AlN phase has the similar periodic lattice structure except the thinner Ti-N layer than Ti_4AlN_3 phase. Through carefully selecting the etching condition (e.g. in 10 wt. % HF for 10 hours), Ti_2AlN nanosheets can also be prepared in our work. Since N atom can be doped into or replace most of carbide MAX phase, it would be an effective strategy to synthesize 2D ternary MAX phase.

Recently, freestanding films have attracted continuing attention due to their potential applications in micro-sensors[30] or energy storage devices.[31] We found that the obtained Ti_4AlN_3 ink could be successfully used to fabricate ultrathin film using Langmuir-Blodgett assembly,[32] as **Figure 3** showed. The as-fabricated Langmuir-Blodgett (LB) film attaching on the PDMS (**Figure 3a**) possesses a good flexibility to bend with the substrate (**Figure 3b**), and it seems semi-transparent. An AFM height measurement (**Figure 3d**) of the film attaching on the silicon wafer (**Figure 3c**) shows that the thickness of Ti_4AlN_3 Langmuir-Blodgett film is only 120 nm, which is comparable to other functional films (e.g. CNT film[33]), and may have the potential in electronic or photonic applications.[10]

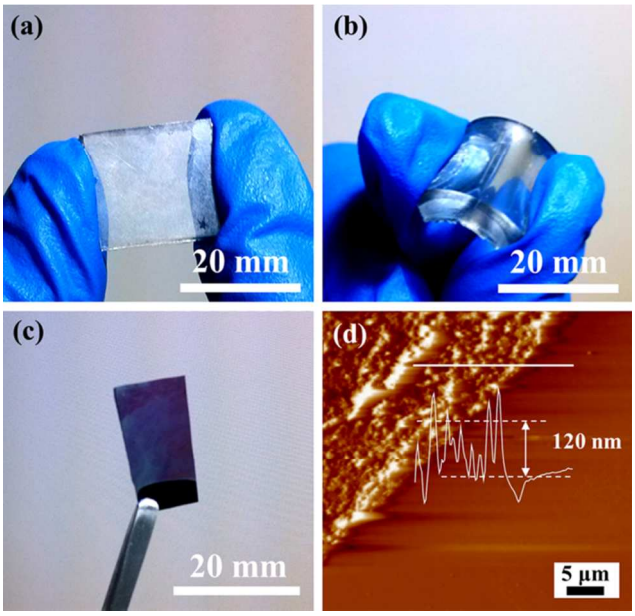

Figure 3. (a, b) Digital photographs of Langmuir-Blodgett (LB) film of Ti_4AlN_3 sheets attaching on the PDMS substrate. (c) Photograph of Ti_4AlN_3 LB film attaching on a Si wafer, and (d) the corresponding AFM measurement of the film.

With the development of UV polymerization, SIPGP has provided a convenient method to grow polymer brushes. In fact, we have successfully functionalized another two-dimension material derived from MAX phase (i.e. V_2C MXene) with PDMAEMA via SIPGP,[25] which endows V_2C to have tunable conductivity during CO_2 uptake and subsequent CO_2 release, and makes the hybrid V_2C as a smart material. Moreover, in order to meet the practical application, we have also fabricated micro-patterns of GO sheets via μCP.[24] The grid patterns with adjustable sizes and shapes are subsequently grafted polystyrene (PS) via SIPGP to achieve patterned polymer brushes, which play an important role in the modification of surface properties.[34, 35] Hence, the functionalization of 2D materials is an effective way to achieve new structures and more properties.

For Ti_4AlN_3 nanosheets, it has shown that they are bearing abundant hydroxyl groups as EDS (**Figure S5b**), FTIR (**Figure S8**) and XPS (**Figure S9**) results indicated. Based on the different hydrogen bond strengths of PDMS-Ti_4AlN_3 and Ti_4AlN_3-silicon interfaces, micro-patterns of Ti_4AlN_3 sheets were easily transferred from PDMS stamp onto Si wafer via μCP, and formed patterns with a size of 10 μm × 10 μm and a thickness of 7 nm (**Figure 4a,** and **4b**) on the substrate. Furthermore, as a photo active site, -OH group on the patterned sheets could be initiated to grow polymer brushes by self-initiated photografting and photopolymerization (SIPGP) from the micro-patterns without a surface bonded initiator.[27] Hence, after immersing the substrate in the styrene monomer solution and irradiating with a UV lamp for an hour, we can grow polystyrene (PS)[24] from Ti_4AlN_3 nanosheets, and achieve functionalized MAX micro-patterns. After polymerization, the resulted thickness is about 160 nm (**Figure 4c,** and **4d**), showing a drastic increase in height, which indicates the successful graft of PS.

In order to achieve more unique nanostructures with special properties, the graft of polymer brushes from MAX sheets cannot be limited to PS or Ti_4AlN_3 phase selected in our work, but should be extended to other polymers or 2D material. This work just opens a door to explore the synthesis of 2D hybrid materials for more functional applications[25, 36] basing on the traditional MAX phases.

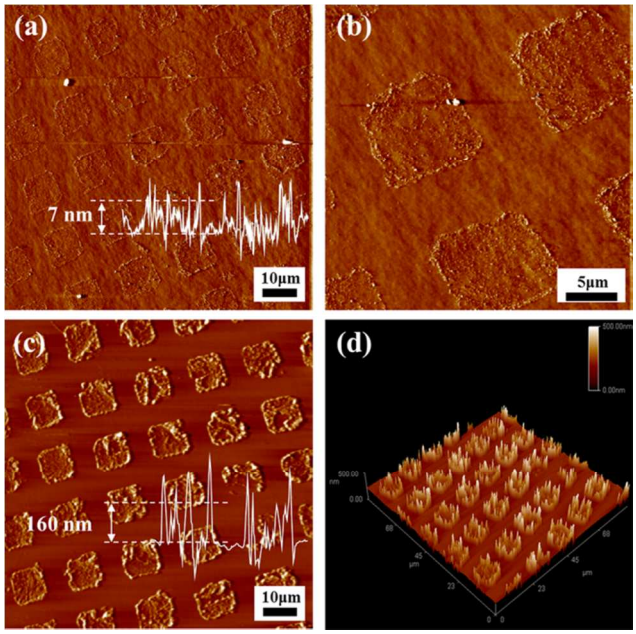

Figure 4. (a) AFM height image of micro-patterned Ti_4AlN_3 nanosheets, and (b) the corresponding amplified image. (c) AFM height image of polystyrene (PS) brushes grafted from micro-patterned Ti_4AlN_3 nanosheets, and (d) the corresponding 3D view.

Conclusions

In summary, a new kind of ternary 2D material, Ti_4AlN_3 phase nanosheets was prepared for the first time through a simple soaking and ultrasonic treating approach. This finding shows that the replacement in the X atom from C to N in MAX phases can dramatically changes their exfoliation behavior in HF solution, and also implicates that more nitride 2D materials can be prepared from their corresponding MAX bulk counterpart. The obtained Ti_4AlN_3 nanosheets containing vast surface groups can be further functionalized to fabricate hybrid patterned polymer brushes through micro-contact printing induced supramolecular self-assembly and subsequent self-initiated photografting and photopolymerization. This micro-patterned MAX-based hybrid system endows the traditional MAX phase to have chemical functionality and more potential applications.

Acknowledgements

This research is supported by National Natural Science Foundation of China (91226202), Ningbo Science and Technology Bureau (2014B82010) and Excellent Youth Foundation of Zhejiang Province of China (LR14B040001).

Notes and references

Qun Ye and Peng Xiao contribute equally.

The authors declare no competing financial interest.

[a]*Ningbo Institute of Material Technology and Engineering, Chinese Academy of Science, Ningbo, People's Republic of China.*

[b]*State Key Laboratory of Nuclear Physics and Technology, Peking University, Beijing, 100871, People's Republic of China.*

**Email: tao.chen@nimte.ac.cn, huangqing@nimte.ac.cn*

Electronic Supplementary Information (ESI) available: [Details of experimental procedures and additional data]. See DOI: 10.1039/b000000x/

1. X. Huang, Z. Y. Yin, S. X. Wu, X. Y. Qi, Q. Y. He, Q. C. Zhang, Q. Y. Yan, F. Boey and H. Zhang, *Small*, 2011, **7**, 1876-1902.
2. L. Lindsay and D. A. Broido, *Phys. Rev. B*, 2011, **84**, 155421.
3. Y. Lin and J. W. Connell, *Nanoscale*, 2012, **4**, 6908-6939.
4. G. Eda, H. Yamaguchi, D. Voiry, T. Fujita, M. W. Chen and M. Chhowalla, *Nano Lett.*, 2011, **11**, 5111-5116.
5. S. Balendhran, J. K. Deng, J. Z. Ou, S. Walia, J. Scott, J. S. Tang, K. L. Wang, M. R. Field, S. Russo, S. Zhuiykov, M. S. Strano, N. Medhekar, S. Sriram, M. Bhaskaran and K. Kalantar-Zadeh, *Adv. Mater.*, 2013, **25**, 109-114.
6. M. Naguib, M. Kurtoglu, V. Presser, J. Lu, J. J. Niu, M. Heon, L. Hultman, Y. Gogotsi and M. W. Barsoum, *Adv. Mater.*, 2011, **23**, 4248-4253.
7. M. W. Barsoum, *Prog. Solid State Chem.*, 2000, **28**, 201-281.
8. Z. M. Sun, *Int. Mater. Rev.*, 2011, **56**, 143-166.
9. P. Eklund, M. Beckers, U. Jansson, H. Hogberg and L. Hultman, *Thin Solid Films*, 2010, **518**, 1851-1878.
10. J. Halim, M. R. Lukatskaya, K. M. Cook, J. Lu, C. R. Smith, L. A. Naslund, S. J. May, L. Hultman, Y. Gogotsi, P. Eklund and M. W. Barsoum, *Chem. Mater.*, 2014, **26**, 2374-2381.
11. M. Ghidiu, M. R. Lukatskaya, M. Q. Zhao, Y. Gogotsi and M. W. Barsoum, *Nature*, **516**, 78-81.
12. M. Naguib, J. Come, B. Dyatkin, V. Presser, P. L. Taberna, P. Simon, M. W. Barsoum and Y. Gogotsi, *Electrochem. Commun.*, 2012, **16**, 61-64.
13. M. Naguib, O. Mashtalir, J. Carle, V. Presser, J. Lu, L. Hultman, Y. Gogotsi and M. W. Barsoum, *Acs Nano*, 2012, **6**, 1322-1331.
14. M. Naguib, J. Halim, J. Lu, K. M. Cook, L. Hultman, Y. Gogotsi and M. W. Barsoum, *J. Am. Chem. Soc.*, 2013, **135**, 15966-15969.
15. M. Ghidiu, M. Naguib, C. Shi, O. Mashtalir, L. M. Pan, B. Zhang, J. Yang, Y. Gogotsi, S. J. L. Billinge and M. W. Barsoum, *Chem. Commun.*, 2014, **50**, 9517-9520.
16. O. Mashtalir, M. Naguib, V. N. Mochalin, Y. Dall'Agnese, M. Heon, M. W. Barsoum and Y. Gogotsi, *Nat. Commun.*, 2013, **4**.
17. M. R. Lukatskaya, O. Mashtalir, C. E. Ren, Y. Dall'Agnese, P. Rozier, P. L. Taberna, M. Naguib, P. Simon, M. W. Barsoum and Y. Gogotsi, *Science*, 2013, **341**, 1502-1505.
18. X. H. Xie, S. G. Chen, W. Ding, Y. Nie and Z. D. Wei, *Chem. Commun.*, 2013, **49**, 10112-10114.
19. X. J. Li, G. Y. Fan and C. M. Zeng, *Int. J. Hydrogen Energ.*, 2014, **39**, 14927-14934.
20. Q. M. Peng, J. X. Guo, Q. R. Zhang, J. Y. Xiang, B. Z. Liu, A. G. Zhou, R. P. Liu and Y. J. Tian, *J. Am. Chem. Soc.*, 2014, **136**, 4113-4116.
21. X. D. Zhang, J. G. Xu, H. Wang, J. J. Zhang, H. B. Yan, B. C. Pan, J. F. Zhou and Y. Xie, *Angew. Chem. Int. Edit*, 2013, **52**, 4361-4365.
22. X. H. Wang and Y. C. Zhou, *J. Mater. Sci. Technol.*, 2010, **26**, 385-416.
23. E. N. Hoffman, D. W. Vinson, R. L. Sindelar, D. J. Tallman, G. Kohse and M. W. Barsoum, *Nucl. Eng. Des.*, 2012, **244**, 17-24.
24. P. Xiao, J. C. Gu, J. Chen, D. Han, J. W. Zhang, H. T. Cao, R. B. Xing, Y. C. Han, W. Q. Wang and T. Chen, *Chem. Commun.*, 2013, **49**, 11167-11169
25. J. Chen, K. Chen, D. Y. Tong, Y. J. Huang, J. W. Zhang, J. M. Xue, Q. Huang and T. Chen, *Chem. Commun.*, 2015, **51**, 314-317.
26. W. L. Liu, *et al*, unpublished work.
27. M. Steenackers, A. Kuller, S. Stoycheva, M. Grunze and R. Jordan, *Langmuir*, 2009, **25**, 2225-2231.
28. J. E. Spanier, S. Gupta, M. Amer and M. W. Barsoum, *Phys. Rev. B*, 2005, **71**, 012103.
29. I. R. Shein and A. L. Ivanovskii, *Comp. Mater. Sci.*, 2012, **65**, 104-114.
30. I. Amin, M. Steenackers, N. Zhang, A. Beyer, X. H. Zhang, T. Pirzer, T. Hugel, R. Jordan and A. Golzhauser, *Small*, 2010, **6**, 1623-1630.
31. Z. Q. Niu, W. Y. Zhou, J. Chen, G. X. Feng, H. Li, W. J. Ma, J. Z. Li, H. B. Dong, Y. Ren, D. A. Zhao and S. S. Xie, *Energ. Environ. Sci.*, 2011, **4**, 1440-1446.
32. L. B. Liu, H. J. Kim and M. Lee, *Soft Matter.*, 2011, **7**, 91-95.
33. W. J. Ma, L. Song, R. Yang, T. H. Zhang, Y. C. Zhao, L. F. Sun, Y. Ren, D. F. Liu, L. F. Liu, J. Shen, Z. X. Zhang, Y. J. Xiang, W. Y. Zhou and S. S. Xie, *Nano Lett.*, 2007, **7**, 2307-2311.
34. B. Zhao and W. J. Brittain, *Prog. Polym. Sci.*, 2000, **25**, 677-710.
35. T. Chen, I. Amin and R. Jordan, *Chem. Soc. Rev.*, 2012, **41**, 3280-3296.
36. J. Chen, P. Xiao, J. C. Gu, Y. J. Huang, J. W. Zhang, W. Q. Wang and T. Chen, *Rsc Adv.*, 2014, **4**, 44480-44485.